

A Subspace-Based Approach to Structural Health Monitoring

Edward C. Larson and B. Eugene Parker, Jr., Ph.D., Barron Associates, Inc., Charlottesville, VA

Abstract

The authors introduce a subspace-based method for tracking structural changes in mechanical systems. Most existing signal processing methodologies in the realm of modal analysis based on vibration signals acquired from accelerometers fail to move beyond merely detecting the existence of changes. Such changes are revealed through departures of modal parameter estimates (eigenfrequencies and mode shape vectors) from baseline values. Much less effort has been devoted to *diagnosing* shifts in modal parameter estimates in terms of changes in mass, stiffness, or damping. In this paper, an advanced approach for detecting and diagnosing (i.e., isolating) changes in aircraft and other mechanical structures is presented. The approach builds upon a broad base of established theoretical methods, including modern spectral analysis (autoregressive, moving-average modeling) techniques for modal parameter estimation and presents a new theoretical approach for diagnostic tracking. The algorithmic methodology is illustrated via simulation of a simple mechanical system. The methods presented lend themselves to nonintrusive, *in situ* monitoring based on natural excitation and are retrofittable to a broad class of existing structures in most immediate need of effective structural health monitoring tools.

Overview

To a perhaps surprising extent, the most common technique for evaluation of structural integrity is still examination with the naked eye during periodic inspections. The examination process has been significantly enhanced in recent decades through the emergence of a host of non-destructive evaluation (NDE) technologies, such as ultrasonic scanning, ground-penetrating radar, thermographic imaging, and eddy-

current probes. However, such technologies are labor- and equipment-intensive; most are impractical for *in situ* monitoring and do not offer the potential for automated operation. Because of the local nature of most NDE technologies, they generally require *a priori* knowledge of where probable damage is located. Although SHM techniques have traditionally focused on *global* – as opposed to local – monitoring of structures, techniques such as those described herein can also be used to monitor damage at localized problem areas (e.g., helicopter fuselage at points of engine attachment). Moreover, most NDE techniques require a direct line of sight to damaged regions and cannot detect damage deep below the surface. SHM, by contrast, implies *in situ* monitoring of the structure with minimal human involvement; in other words, the ability to monitor the structure continuously during usage, without need for disassembly or (necessarily) *a priori* knowledge of where damage will likely occur.

The most questionable aspect of vibration monitoring/modal analysis is that, when used for global monitoring of structural health, it relies on long wavelengths (comparable to the dimensions of the entire structure) that are several orders of magnitude greater than the dimensions of small cracks that characterize incipient faults. Ultrasonic interrogation, by contrast, utilizes wavelengths comparable to or smaller than crack dimensions. This concern about vibration monitoring, which may limit detection to widespread fatigue damage, has been raised frequently in the literature and is indeed germane.

There are several responses to such arguments. First, vibration monitoring can be performed locally (rather than globally), such as to monitor for damage at *a priori* known problem areas, as is commonly done with other methods. Indeed, the SHM methods

described herein can operate using many of the new sensor technologies (e.g., fiber-optic accelerometers and displacement sensors) that are being considered for retrofit and forward-fit (e.g., embedded composites) SHM applications. Even if non-vibration techniques (e.g., ultrasonics, acoustic emission) do prove to be inherently superior for incipient crack detection on physical grounds, there is still a place for vibration monitoring. All of the aforementioned advantages – low cost, low power, nonintrusiveness, *in situ* operating capability, retrofit capability, ease of comprehending the underlying physics and interpreting data – still apply.

For global monitoring, which is generally not performed with other methods, it is known that eigenfrequency values change relatively little until damage reaches near-critical levels. However, mode shapes are much more sensitive and informative indicators of early damage. Identifying mode shapes requires either very sensitive displacement detection (e.g., using lasers or optical interferometers) or densely spaced sensors. With moderately spaced sensors, global vibration monitoring most likely cannot detect incipient faults in their earliest stages, but it is likely to catch such faults well before they become critical. With fewer sensors, one merely has less resolution concerning mode shape than is desired. As long as damage can be detected well before it jeopardizes safety, vibration monitoring can make a valuable contribution. Indeed, vibration-based SHM can be used in conjunction with NDE and visual inspections, acting as a sentinel in-between scheduled manual inspections to increase the margin of safety. It is noted that aircraft aeroelasticity models can be taken into consideration in the vibration monitoring algorithms to improve their sensitivity and specificity in detecting only structural changes that are of interest and to aid in establishing detection thresholds pertaining to structural damage.

Improved measurement of acceleration and displacement, such as through optical sensing technologies, will provide increased sensitivity to low-level structural vibration. This will enable superior mode-shape resolution than is possible using more conventional piezoelectric accelerometer technologies. Op-

tical techniques, such as laser Doppler vibrometry and fiber-optic Bragg grating arrays, are immune from electromagnetic interference (EMI), which results in much greater signal-to-noise ratio and therefore high sensitivity to low-amplitude surface vibration. This is especially important in natural excitation scenarios, in which most external excitation is of very low power. Another advantage of optical vibration monitoring is that it provides orders of magnitude improvement in spatial (and temporal) resolution compared to discrete piezoelectric accelerometers, due to the short wavelengths of visible light. This can potentially facilitate detection of modal perturbation effects that arise from localized, incipient damage. Moreover, some fiber-optic sensors can provide continuous spatial information; achievement of similar capability with piezoelectric accelerometers would require many densely spaced sensors. The theoretical results for vibration-based SHM presented in this paper are applicable to both low- and high-end measurement technologies.

There is still much unexplored ground and room for continuing progress and new ideas in the field of modal analysis. The work presented herein was pursued largely in this spirit. Advanced signal processing and inference-based approaches for structural health assessment provide, in addition to mathematical tools and theoretical insights, a vision and a strategic link between manual NDE technologies and automated SHM. Some of the concepts emerging from this work may be indirectly applicable to non-vibration monitoring technologies, such as acoustic emission or ultrasonic-based electromechanical impedance.

Research Thrusts in Structural Health Monitoring

One very important high-level issue that has received relatively little attention in SHM circles is retrofit capability. Life extension is clearly a dominant objective of SHM, but the most heavily emphasized areas in the SHM field today (e.g., judging from the contents of [2]) appear to be geared toward such trends as specialized composite materials, self-repairing materials, and smart micro-electromechanical systems

(MEMS)-based structures. Quite obviously, a great many existing structures (e.g., bridges, commercial aircraft) do not contain such advanced materials and sensor technologies. For this reason, aging structures in greatest need of effective health monitoring stand to benefit *least* from the preponderance of SHM research that is being pursued today.

That vibration monitoring lends itself to retrofit is an additional reason for our focus on such. Accelerometers are inexpensive, relatively small, and noninvasive. They can be mounted on structures at more or less arbitrary locations, which makes it possible to monitor parts of a structure that are inaccessible to direct inspection. Furthermore, as a passive monitoring technique not requiring actuation (i.e., does *not* require an excitation signal to interrogate the structure), vibration monitoring consumes very little power and presents minimal disruption during in-service operation.

Algorithms for vibration monitoring are the focus of the present paper. In addition to the reasons given above, vibration monitoring is the most mature and least expensive of the aforementioned physical technologies. It is well-established in the literature (see [3]) and widely applied in many civil infrastructure and aerospace realms. Unlike for most other monitoring technologies, there is a considerable amount of data (e.g., I-40 bridge data acquired at Los Alamos National Laboratory [5]) against which new algorithms can be tested.

Furthermore, the underlying physics of modal analysis is well-developed, relatively simple, and completely general. In contrast with some other physical approaches, it is not limited to certain types of materials (e.g., electrically conductive or layered-composites). It is straightforward to formulate the signal processing and system identification aspects of the damage detection/identification problem in clear-cut manners. Pattern recognition tasks, unlike with acoustic emission or ultrasonic interrogation, are relatively straightforward. The use of first-principles mechanical models implies that fault severity assessment can be formulated in a quantitative and readily interpretable manner. Model-based damage detection and isolation is the method

of choice when physical models of mechanical systems are available and practicable, as they are herein.

Natural versus Artificial Excitation

In vibration monitoring applications, there is an important distinction between artificial and natural excitation. Most prior experimental work in modal analysis involves the former, in which the structure is interrogated with known excitation forces produced by an artificial shaker. Use of shakers is an equipment-intensive and intrusive process; it is impractical for most *in situ* monitoring scenarios. *Our focus herein will be on structural diagnostics wherein only the natural, unmeasured, and unknown excitations (e.g., wind, turbulence, waves, etc.) act to excite the structure.*

Natural excitation appropriately pertains to most practical SHM applications, in which excitation forces are unmeasured and unknown. However, the signal processing problem becomes much more complicated. Whereas artificial excitation involves straightforward system identification of the transfer function, $\tilde{G}_{yf}(\omega)$ (introduced in detail later on), the signal processing challenge with natural excitation is one of *blind deconvolution*. This requires certain assumptions about the statistical behavior of the excitation forces, as is discussed in Section .

Diagnostic Monitoring of Vibrating Structures

In this section we focus on fundamental information-theoretic questions concerning vibration-based SHM. The chief question is: What is the maximum amount of information that can be extracted from vibration monitoring of a mechanical structure? The short answer is that the *modal parameters* of the system (which in this context are reflective not only of the mechanical system, but also of the configuration of the sensor array) constitute essentially all of the information that can be obtained through vibration monitoring. Here we are concerned with the higher-level question of to what end complete and perfect knowledge of the modal parameter values should be used. It is well-known that, in practice, the modal parameters do not uniquely determine the underlying health condition of a mechanical system, in terms

of directly relevant and comprehensible properties such as mass, stiffness, and damping parameters. In this section we show how modal parameter estimates can be used for purposes of diagnostics (i.e., damage isolation), in addition to detecting the existence of structural change.

Simplified Physical Modeling for Vibration-Based SHM

From a physical viewpoint, any extended mechanical structure can be modeled as a lattice of interacting point-mass particles. In a simple mass-spring-damper model, the vibrational motion is governed by a system of linear equations of the general form

$$\mathbf{m}\ddot{\underline{X}} + \mathbf{b}\dot{\underline{X}} + \mathbf{k}\underline{X} = \underline{f}(t), \quad (1)$$

in which \underline{X} is an $N \times 1$ vector of lumped-element displacements (where N is the total number of mass elements). \mathbf{m} , \mathbf{b} , and \mathbf{k} are $N \times N$ matrices representing, respectively, the distributions of mass, dissipative damping, and elasticity in the system. It should be recognized that Eq. 1 is a reduced-order model. N should not be regarded as a fixed, well-defined number; it is indefinitely large. In general, it can be expected that there exists a family of mechanical models of the form in Eq. 1 that can accurately account for the observed behavior of the actual system. Methods for establishing an adequate model in this regard are available [1].

Eq. 1 can be cast into a canonical first-order form by treating particle displacements and velocities as states, *viz.*,

$$\underline{x} \equiv \begin{pmatrix} \underline{X} \\ \dot{\underline{X}} \end{pmatrix}. \quad (2)$$

Eq. 1 then assumes the form

$$\dot{\underline{x}} = \mathbf{A}\underline{x} + \mathbf{B}\underline{f}(t) \quad (3)$$

in which

$$\mathbf{A} \equiv \begin{pmatrix} \mathbf{0}_{N \times N} & \mathbf{1}_{N \times N} \\ -\mathbf{m}^{-1}\mathbf{k} & -\mathbf{m}^{-1}\mathbf{b} \end{pmatrix} \quad (4)$$

$$\mathbf{B} \equiv \begin{pmatrix} \mathbf{0}_{N \times N} \\ \mathbf{m}^{-1} \end{pmatrix}.$$

The \mathbf{A} matrix can be diagonalized, *viz.*,

$$\mathbf{A} = \boldsymbol{\lambda}^{-1} \mathbf{A}_m \boldsymbol{\lambda} \quad (5)$$

in which \mathbf{A}_m is a diagonal matrix of eigenfrequencies and $\boldsymbol{\lambda}$ is a transformation matrix between mass-element coordinates (in which Eq. 1 is formulated) and modal coordinates.

The sensor outputs usually represent displacements (doubly-integrated accelerations) at certain locations on the structure. The output vector, \underline{y} , from the sensor array may be modeled as a linear combination of the system states, *viz.*,

$$\underline{y} = \mathbf{C}\underline{x}. \quad (6)$$

The number of rows in \underline{y} and \mathbf{C} is equal to the number of sensor channels, denoted as R . Unlike N , R is a well-defined and relatively small number ($R \cdot N$ may always be assumed). The sensor configuration matrix, \mathbf{C} , can be deduced from knowledge of the sensor placements vis-à-vis the geometrical shape of the object. In modal coordinates, the matrix

$$\mathbf{C}_m = \mathbf{C}\boldsymbol{\lambda}^{-1} \quad (7)$$

contains the mode shape coefficients.

Embedment of Modal Parameters in the Power Spectrum

From the sensor output time-series data, one can compute the spectral density, or power spectrum, henceforth denoted as $\tilde{\chi}_{yy}(\omega)$. The spectral density, which is an $R \times R$ matrix, contains all of the second-order statistical information embedded in the system. It can readily be shown, analytically, that the spectral density is equal to

$$\tilde{\chi}_{yy}(\omega) = \tilde{\mathbf{G}}_{yf}(\omega) \boldsymbol{\Sigma}_{ff} \tilde{\mathbf{G}}_{yf}^\dagger(\omega) \quad (8)$$

in which ‘ \dagger ’ denotes the conjugate transpose and

$$\tilde{\mathbf{G}}_{yf}(\omega) = \mathbf{C}_m(i\omega - \mathbf{A}_m)^{-1} \quad (9)$$

is the transfer function from the excitation forces (strictly speaking, the second term on the right-hand side of Eq. 3) to the sensor outputs, and $\boldsymbol{\Sigma}_{ff}$ is the force covariance matrix. It follows that if $\tilde{\chi}_{yy}(\omega)$

is completely known, \mathbf{A}_m (i.e., the eigenfrequencies) and \mathbf{C}_m (i.e., the mode shape coefficients) can, in principle, both be ascertained via analytic continuation. Estimating \mathbf{A}_m and \mathbf{C}_m represent the objectives of the signal processing tasks. There are a number of well-established algorithmic methods, based on modern spectral estimation techniques (e.g., [1]), for extracting modal parameter estimates numerically from empirically-measured accelerometer data. We will not review these techniques here, since our focus is not on measuring them but rather on how they can be used for purposes of diagnostic assessment.

Extension to White Nonstationary and Non-White Stationary Excitation

It was noted above that vibration monitoring in a natural excitation context is tantamount mathematically to blind deconvolution, which requires certain statistical assumptions about the input excitation. In many actual operating environments, the forces can be regarded, to a high degree of realism, as being stochastically white. In these cases, the expression for the spectral density in Eq. 8 is rigorously valid. Moreover, the modal parameter estimates derived from measured spectral density are independent of the force covariance.

The case of white, nonstationary excitation means that Eq. 8 still applies, except that the force covariance matrix, $\mathbf{\Sigma}_{ff}$, is time-varying. Because the modal parameter estimates, $(\mathbf{A}_m, \mathbf{C}_m)$, are independent of the covariance, however, it follows that these estimates remain constant (in the absence of any underlying structural change) despite the time variation of the excitation covariance.

If the excitation forces are non-white, or *colored*, the only difference is that Eq. 8 must be modified slightly. One must replace the force-output transfer function $\tilde{\mathbf{G}}_{yf}(\omega)$ with the composite expression

$$\tilde{\mathbf{G}}_{y\nu}(\omega) \equiv \tilde{\mathbf{G}}_{yf}(\omega)\tilde{\mathbf{G}}_{f\nu}(\omega). \quad (10)$$

The excitation is modeled as a causal filtering of white noise and is represented by the transfer function $\tilde{\mathbf{G}}_{f\nu}(\omega)$. The objective is to isolate the structural transfer function, $\tilde{\mathbf{G}}_{yf}(\omega)$.

The set of poles of the combined transfer function, $\tilde{\mathbf{G}}_{y\nu}(\omega)$, which determines $\tilde{\chi}_{yf}(\omega)$, is a composite of the structural poles, of $\tilde{\mathbf{G}}_{yf}(\omega)$, and those of the coloration filter, $\tilde{\mathbf{G}}_{f\nu}(\omega)$. Spectral separation of the two sets of poles is possible if $\tilde{\mathbf{G}}_{yf}(\omega)$ and $\tilde{\mathbf{G}}_{f\nu}(\omega)$ are very different in their morphological features. Structural transfer functions generally have a number of narrow resonance peaks. If the coloration filter does not possess sharp resonance peaks (this is true, for example, in aircraft turbulence and gust models [4]) for example, the combined transfer function will still possess sharp peaks at the structural pole locations. Essentially all that will be altered are the relative peak amplitudes.

In the present context, natural excitation and blind deconvolution therefore require only mild assumptions about the statistical behavior of the excitation forces.

Linkage Between Modal- and Mass-Element Coordinates

With knowledge of the modal parameters, \mathbf{A}_m and \mathbf{C}_m , we next want to know how to extract diagnostic information about the mechanical system. More specifically, we wish to deduce the \mathbf{A} matrix in Eqs. 3 and 4, which would amount to a complete solution of the diagnostics problem, since \mathbf{A} contains full information about the mass, stiffness, and damping properties of the system.

Diagnosing a mechanical system requires that the state dynamics matrix in mass-element coordinates, \mathbf{A} be identified, which implies that the λ matrix in Eq. 5 must be identified. One link from modal coordinates, in which all of the signal processing analysis has been done, to mass-element coordinates, is furnished by Eq. 7. The sensor configuration matrix, \mathbf{C} , which is in the mass-element coordinate frame, can be deduced based on knowledge of the sensor placements vis-à-vis the geometrical shape of the object and the mechanical model, *viz.*,

$$\mathbf{C}_m\lambda = \mathbf{C}. \quad (11)$$

A second equation akin to Eq. 11 is the following:

$$\mathbf{C}_m\mathbf{A}_m\lambda = \mathbf{C}_m\lambda\lambda^{-1}\mathbf{A}_m\lambda$$

$$\begin{aligned}
&= \mathbf{C}\mathbf{A} \\
&= (\mathbf{C}_t \mathbf{0}_{R \times N}) \begin{pmatrix} \mathbf{0}_{N \times N} & \mathbf{1}_{N \times N} \\ -\mathbf{m}^{-1}\mathbf{k} & -\mathbf{m}^{-1}\mathbf{b} \end{pmatrix} \\
&= (\mathbf{0}_{R \times N} \mathbf{C}_t) \quad (12)
\end{aligned}$$

in which \mathbf{C}_t is the *truncated* sensor configuration matrix, consisting of the first N columns of \mathbf{C} . The final step in Eq. 12 is based on the fact that only the first N columns of \mathbf{C} contain nonzero values. In mass-element coordinates, this condition can be stipulated without loss of generality, since the first N columns correspond to displacement degrees of freedom in the mechanical system, whereas columns $N + 1$ to $2N$ correspond to velocities.

Eqs. 11 and 12 can be combined into a single matrix equation, *viz.*,

$$\begin{pmatrix} \mathbf{C}_m \\ \mathbf{C}_m \mathbf{A}_m \end{pmatrix} \boldsymbol{\lambda} = \begin{pmatrix} \mathbf{C}_t & \mathbf{0}_{R \times N} \\ \mathbf{0}_{R \times N} & \mathbf{C}_t \end{pmatrix}. \quad (13)$$

This yields $2N$ systems of linear equations for the columns of $\boldsymbol{\lambda}$. Assuming that the stacked matrix on the left-hand side of Eq. 13 is full-rank (which will be the case if the sensors are mutually independent and non-collocated), this implies $2R$ equations in $2N$ unknowns for each column of $\boldsymbol{\lambda}$.

One corollary of Eq. 13 is that $\boldsymbol{\lambda}$ can be determined uniquely if and only if $R = N$, i.e., if one sensor is available for every single mass element in the mechanical structure. Alternatively interpreted, the stacked matrix on the left-hand side in that case is an invertible square matrix, whence one can readily solve for $\boldsymbol{\lambda}$. Having determined $\boldsymbol{\lambda}$, the state dynamics matrix can then be estimated as

$$\begin{aligned}
\hat{\mathbf{A}} &\equiv \boldsymbol{\lambda}^{-1} \mathbf{A}_m \boldsymbol{\lambda} \\
&= \mathbf{A}. \quad (14)
\end{aligned}$$

In conclusion, it is possible, in the case of $R = N$, to deduce \mathbf{A} .

Linear Subspace Partitioning of $\boldsymbol{\lambda}$

In practical SHM applications, the assumption of $R = N$ is, of course, unrealistic. The number of available sensors is almost always less than the number of degrees of freedom in the mechanical system.

Henceforth, we focus on the case of $R < N$, in which case only partial mode shape information is available. Eq. 13 becomes an under-determined system, which indicates that $\boldsymbol{\lambda}$ cannot be determined uniquely. However, partial information about $\boldsymbol{\lambda}$ is still available. It is noted that even in the extreme case of just a single sensor ($R = 1$), a small amount of mode shape information exists solely by virtue of knowledge of where the sensor is located.

For $R < N$, any $\boldsymbol{\lambda}$ matrix satisfying Eq. 13 is of the form

$$\boldsymbol{\lambda} = \boldsymbol{\lambda}_\perp + \boldsymbol{\lambda}_\parallel \boldsymbol{\beta} \quad (15)$$

in which $\boldsymbol{\lambda}_\perp$ is a $2N \times 2N$ matrix whose column eigenspace, which is of dimension $2R$, is known as the *row space* of the system (which encompasses both the mechanical system model and the sensor array configuration). $\boldsymbol{\lambda}_\perp$ can readily be computed explicitly, *viz.*,

$$\boldsymbol{\lambda}_\perp \equiv \begin{pmatrix} \mathbf{C}_m \\ \mathbf{C}_m \mathbf{A}_m \end{pmatrix}^+ \begin{pmatrix} \mathbf{C}_t & \mathbf{0}_{R \times N} \\ \mathbf{0}_{R \times N} & \mathbf{C}_t \end{pmatrix} \quad (16)$$

in which ‘+’ denotes the Moore-Penrose pseudoinverse. $\boldsymbol{\lambda}_\parallel$ is a $2N \times 2(N - R)$ matrix whose column eigenspace, known as the *null space* of the system, is the orthogonal complement of the row space. The null space is of dimension $2(N - R)$. Pairs of rows in the resulting $\boldsymbol{\lambda}_\perp$ and $\boldsymbol{\lambda}_\parallel$ matrices are complex-conjugates of one another. $\boldsymbol{\beta}$ is a real-valued $2(N - R) \times 2N$ matrix all of whose elements are indeterminate.

Nonlinear Constraints on $\boldsymbol{\beta}$

The final conclusion from above is that the set of potential state dynamics matrices, \mathbf{A} , and transformation matrices, $\boldsymbol{\lambda}$, from mass-element to modal coordinates can be represented by means of a $4N(N - R)$ -dimensional space of real-valued $\boldsymbol{\beta}$ matrices. For any particular $\boldsymbol{\beta}$ matrix in this space, $\boldsymbol{\lambda}$ can be computed via Eq. 15, and $\hat{\mathbf{A}}$ can be then be computed as

$$\hat{\mathbf{A}}(\boldsymbol{\beta}) \equiv [\boldsymbol{\lambda}(\boldsymbol{\beta})]^{-1} \mathbf{A}_m \boldsymbol{\lambda}(\boldsymbol{\beta}). \quad (17)$$

However, not all $\hat{\mathbf{A}}$ matrices obtained in this manner are consistent with the known form of the actual

state dynamics matrix, \mathbf{A} , in Eq. 4. The most obvious requirement is that the upper half of $\hat{\mathbf{A}}$ consist only of zeros and ones in the fashion indicated in Eq. 4. As a result, the subset of admissible β matrices is a *nonlinear manifold* embedded in a real space of dimension $4N(N - R)$. The nonlinearity is due to the matrix inverse in Eq. 17.

Diagnostic Tracking of Observed Structural Change

If the system is monitored over a long period of time, small changes in \mathbf{A}_m and \mathbf{C}_m may be observed due to underlying changes in the structural condition (which is embodied mathematically in the mass, stiffness, and damping matrices in Eq. 1). It is noted that some changes (e.g., a diminution in stiffness) may be health-related, whereas other types of structural change (e.g., a change in mass due to fuel expenditure) are not. For this and other reasons, the ability to diagnose observed changes in the modal parameter set, $(\mathbf{A}_m, \mathbf{C}_m)$, is of major practical interest.

In the diagnostic tracking approach developed by the authors, small observed changes in $(\mathbf{A}_m, \mathbf{C}_m)$ are accompanied by small, continuous changes in β and in the resulting estimate of the \mathbf{A} matrix, per Eq. 17. It is possible to update β , in a manner consistent with the aforementioned nonlinear constraints, in such a way that the change in \mathbf{A} is minimized (with respect to some matrix norm). The resulting β path then provides the most parsimonious explanation for the observed changes in \mathbf{A}_m and \mathbf{C}_m . In other words, it answers the question: What is the least amount of change in \mathbf{A} that is consistent with the observed modal parameter shifts?

Example of Diagnostic Tracking

As an application example, the updating method is applied to a simple mechanical model depicted in Fig. 1. In this system, $N = 3$, $R = 1$, and the undamaged condition is given by

$$\mathbf{m} = \begin{pmatrix} 1 & 0 & 0 \\ 0 & 1 & 0 \\ 0 & 0 & 1 \end{pmatrix} \quad \mathbf{k} = \begin{pmatrix} 2 & -1 & 0 \\ -1 & 2 & -1 \\ 0 & -1 & 2 \end{pmatrix} \quad (18)$$

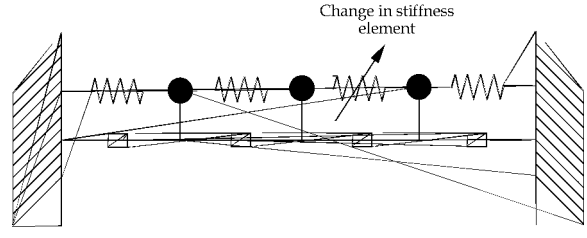


Figure 1: Simulation of Damage in a Simplified Mechanical System Model

$$\mathbf{b} = \begin{pmatrix} 0.2 & -0.1 & 0 \\ -0.1 & 0.2 & -0.1 \\ 0 & -0.1 & 0.2 \end{pmatrix}.$$

\mathbf{m} , \mathbf{k} , and \mathbf{b} are respectively the mass, stiffness, and damping matrices. To simulate damage, the stiffness element k_{23} and its mirror image, k_{32} , are reduced from -1 to -0.99 . The final condition is therefore

$$\mathbf{m} = \begin{pmatrix} 1 & 0 & 0 \\ 0 & 1 & 0 \\ 0 & 0 & 1 \end{pmatrix} \quad \mathbf{k} = \begin{pmatrix} 2 & -1 & 0 \\ -1 & 2 & -0.99 \\ 0 & -0.99 & 2 \end{pmatrix} \quad (19)$$

$$\mathbf{b} = \begin{pmatrix} 0.2 & -0.1 & 0 \\ -0.1 & 0.2 & -0.1 \\ 0 & -0.1 & 0.2 \end{pmatrix}.$$

This diminution of stiffness results in changes in the observed \mathbf{A}_m and \mathbf{C}_m matrices. If the path from the initial to final $(\mathbf{A}_m, \mathbf{C}_m)$ is discretized into 100 steps and the updating algorithm is implemented, the resulting estimates of \mathbf{m} , \mathbf{b} , and \mathbf{k} (normalized with respect to the first mass) are

$$\mathbf{m} = \begin{pmatrix} 1.0000 & 0 & 0 \\ 0 & 1.0014 & 0 \\ 0 & 0 & 1.0010 \end{pmatrix} \quad \mathbf{k} = \begin{pmatrix} 1.9998 & -1.0005 & -0.0002 \\ -1.0005 & 2.0026 & -0.9914 \\ -0.0002 & -0.9914 & 2.0025 \end{pmatrix} \quad (20)$$

$$\mathbf{b} = \begin{pmatrix} 0.1999 & -0.1004 & -0.0001 \\ -0.1004 & 0.2004 & -0.0998 \\ -0.0001 & -0.0998 & 0.2002 \end{pmatrix}$$

which are in reasonably good agreement with Eq. 19. k_{23} and k_{32} are the element pair that exhibits the

largest relative jump. Hence, the technique not only succeeds in detecting structural change, but also provides information about the location, nature, and severity of the fault. It indicates that it is due to a change in stiffness, as opposed to mass or damping, that it involves the 2-3 mass pair, and that the magnitude of stiffness reduction is approximately 0.86%.

Once such a diagnostic inference has been made, a more precise characterization of the change can be obtained by introducing additional constraints on β . For example, if it is surmised or known that the structural change involves only the stiffness, the lower right-hand quadrant of the estimated state transition matrix, $\hat{\mathbf{A}}$, can be held fixed by reducing the space of admissible β paths. The resulting final estimate of the stiffness matrix is then

$$\mathbf{k} = \begin{pmatrix} 1.9998 & -0.9999 & 0.0002 \\ -0.9999 & 1.9997 & -0.9901 \\ 0.0002 & -0.9901 & 2.0005 \end{pmatrix} \quad (21)$$

which is more accurate (estimated stiffness reduction is 0.99%).

Conclusions

We have investigated advanced signal processing methodologies that pertain directly to SHM of aircraft and other mechanical structures. The methods are based on natural, rather than artificial, excitation and are insensitive to the excitation noise characteristics, which is important in making the techniques practical for *in situ*, round-the-clock monitoring. Subspace-based modal parameter estimation algorithms have been applied successfully in the SHM context, and we have shown that they hold promise for detecting incipient damage. We have devised and presented preliminary results for a new theoretical approach that makes it possible to diagnose observed modal parameter shifts in terms of mass, stiffness, and damping elements in underlying mechanical models of structures. Subsequent work is planned to demonstrate the techniques using real-world sensor data collected on structures at the NASA Langley Research Center.

References

- [1] Basseville, M., A. Benveniste, B. Gach-Devauchelle, M. Goursat, D. Bonnecase, P. Dorey, M. Prevosto, and M. Olagnon, "In situ damage monitoring in vibration mechanics: diagnostics and predictive maintenance," *Mechanical Systems and Signal Processing*, Vol. 7, No. 5, 1993, pp. 401-423.
- [2] Chang F.K., ed., *Proc. of the 2nd International Workshop on Structural Health Monitoring*, Stanford Univ., Stanford, CA, Sep. 1999.
- [3] Doebling, S.W., Farrar, C., Prime, M.B., and D.W. Shevitz, "Damage Identification and Health Monitoring of Structural and Mechanical Systems from Changes in their Vibration Characteristics: A Literature Review." Technical Report LA-13070-MS, Los Alamos National Laboratory, Los Alamos, NM, 1996.
- [4] Hoblit, F.M., *Gust Loads on Aircraft: Concepts and Applications*, J.S. Przemieniecki, ed., Washington DC, AIAA, 1988.
- [5] http://www.lanl.gov/damage_id/home.htm.

Acknowledgments

This investigation was funded by the NASA Langley Research Center (LaRC) under the auspices of the NASA Aviation Safety Program (AvSP), as part of the Single Aircraft Accident Prevention (SAAP) thrust, via Lockheed Martin (LM) Tactical Aircraft Systems (Ft. Worth, TX) Affordable Integrated Management Systems for Aviation Flight Safety Enhancement (AIMSAFE) P.O. 7039386. The authors thank Dr. Celeste M. Belcastro and Dr. Christine M. Belcastro of the NASA LaRC and Dr. Rowena L. Eberhardt of LM for their support of this work.